Synthesis and Solubility of Linear Poly(tetrafluoroethylene-*co*-vinyl acetate) in Dense CO_2: Experimental and Molecular Modeling Results

Bilal Baradie and Molly S. Shoichet

Department of Chemical Engineering and Applied Chemistry, University of Toronto, 200 College Street, Toronto, Ontario, Canada M5S 3E5, and Department of Chemistry, University of Toronto, 80 St. George Street, Toronto, Ontario, Canada M5S 1A1

Zhihao Shen and Mark A. McHugh

Department of Chemical Engineering, Virginia Commonwealth University, 601 West Main Street, Richmond, Virginia 23284

Lei Hong, Yang Wang, J. Karl Johnson, Eric J. Beckman, and Robert M. Enick*

Department of Chemical Engineering, 1249 Benedum Hall, University of Pittsburgh, Pittsburgh, Pennsylvania 15261

Received March 29, 2004; Revised Manuscript Received July 8, 2004

ABSTRACT: Supercritical carbon dioxide was used as a reaction medium to synthesize statistically random (i.e., no specific correlation between the location of the monomers on the polymer) copolymers of tetrafluoroethylene (TFE) and vinyl acetate (VAc) with similar molar mass and 11.6−63.3 mol % TFE content. The solubility of the copolymers at 25 °C in CO_2 reduced after reaching a maximum value at a TFE molar concentration of 19.3 mol %. The 46.7 mol % TFE copolymer only dissolved in CO_2 at elevated temperatures, whereas the 63.3 mol % TFE copolymer did not dissolve in CO_2 even at temperatures in excess of 144 °C and pressures of 210 MPa. The molecular modeling results show that the interaction of CO_2 with acetate side group was not affected by presence of fluorine in the polymer backbone; therefore, the enhanced solubility of the semifluorinated copolymers is attributable to the enhanced binding between CO_2 and the semifluorinated backbone of the copolymer when the CO_2 molecule can access both the fluorinated (Lewis base) and hydrogenated (Lewis acid) parts of the backbone simultaneously.

Introduction

Poly(tetrafluoroethylene-*co*-vinyl acetate) (poly(TFE-*co*-VAc)) is a fluoropolymer with potential applications in the coatings, optical, and biomedical fields.[1−3] Poly(TFE-*co*-VAc) can be synthesized via free radical copolymerization of tetrafluoroethylene (TFE) and vinyl acetate (VAc) in dense carbon dioxide, with the composition of the TFE−VAc copolymer being controlled by the ratio of monomers in the feed.[4] Although a small concentration of fluoro surfactant is added to the monomers and CO_2 in an initial study of this polymerization, subsequent trials without surfactant yielded copolymers of similar polydispersity and greater molar mass, implying that the surfactant is not necessary for solubility of the macroradical chains.[5] On the basis of reactivity ratios, poly(TFE-*co*-VAc) is a random copolymer because TFE cross-propagates with VAc, and VAc propagates in such a manner that the sequence of VAc and TFE units in the polymer backbone is randomly ordered (i.e., these polymers are not diblock copolymers composed of a long chain of perfluoroethylene joined to a long chain of poly(vinyl acetate)). Hydrolysis of VAc to vinyl alcohol (VA) yields the predicted decrease in copolymer molar mass to form poly(TFE-*co*-VAc-*co*-VA), suggesting that the copolymer was linear.[4,5] This is in contrast to poly(TFE-*co*-VAc) prepared by emulsion, where a precipitous drop in molar mass is observed upon hydrolysis due to ester groups in the backbone. The high yield and high molar mass of the TFE−VAc copolymers provide indirect evidence that poly(TFE-*co*-VAc) is CO_2-soluble at reaction conditions of 45 °C and 20−23 MPa and loadings of 20% w/v. Because the polymerization was conducted in a vessel that did not permit detection of the phase behavior, the actual CO_2 solubility of these polymers was not determined.

The phase behaviors of the homopolymers of each monomer have been previously established. Poly(vinyl acetate), PVAc, is a noncrystalline, low-T_g (glass transition temperature) polymer that exhibits the greatest degree of CO_2 solubility associated with any high molecular weight oxygenated hydrocarbon homopolymer that has yet been identified, although it is far less CO_2-philic than fluoroacrylate or siloxane-based polymers.[6,7] This high degree of CO_2 solubility has been attributed to a weak complex that forms between CO_2 and the readily accessible acetate group.[6,7] PTFE is a crystalline polymer that is insoluble in CO_2 and organic solvents, although it does dissolve at high temperatures in high molecular weight fluorocarbon solvents.[8] Poly(tetrafluoroethylene-*co*-19.3 mol % hexafluoropropylene) (FEP_{19}) is a nonpolar fluorocopolymer that has similar properties to PTFE, but FEP_{19} is highly branched and therefore has normal melting point at ∼145 °C, whereas PTFE has a melting point in excess of 300 °C. It has been demonstrated that FEP_{19} can dissolve in supercritical CO_2 at temperatures in excess of 185 °C and pressures of approximately 100 MPa.[8−10] If the TFE segments in FEP_{19} are replaced with vinylidene fluoride (VF), this VF−HFP copolymer remains in solution to very low temperatures since the polar character of the VF group interacts with the quadrupole of CO_2.[11] These

* Corresponding author: Tel (412) 624−9649, Fax (412) 624-9639, e-mail enick@engrng.pitt.edu.

10.1021/ma049384u CCC: $27.50
Published on Web 08/27/2004

phase behavior results suggested that perfluorination does not impart polymers high solubility in CO_2. This argument had also been made by Raveendran et al. through molecular simulation; i.e., partially fluorinated molecules provide more favorable binding sites for CO_2 than perfluorinated analogues.[12]

The objective of this study is to experimentally establish whether random copolymers of TFE and VAc are indeed CO_2-soluble at levels in excess of those exhibited by PVAc homopolymer containing a comparable number of repeat units. Poly(TFE-*co*-VAc) samples are prepared by radical copolymerization in supercritical CO_2 without surfactants, and the phase behavior of the copolymers is measured using nonsampling techniques in windowed, variable-volume cells. If the TFE−VAc copolymers are indeed more CO_2-soluble than homopolymers of VAc, then molecular modeling will be used to characterize the CO_2−polymer interactions in the CO_2−PVAc and CO_2−poly(TFE-*co*-VAc) systems.

Experimental Section

Reagents. All chemicals were purchased from Aldrich (Ontario, Canada) and used as received unless otherwise specified. TFE was prepared by vacuum pyrolysis of PTFE[13] and stored at room temperature over d-limonene in a 300 mL stainless steel sample cylinder fitted with an 12.4 MPa safety rupture disk. [Caution: tetrafluoroethylene is inherently dangerous, and anyone contemplating handling TFE under high pressures should be very familiar with safe handling procedures.] TFE-*co*-VAc copolymers were synthesized as previously described,[5] with the only difference being the compositions synthesized. As previously described, polymers were synthesized without a surfactant and by radical copolymerization in supercritical fluid CO_2 using diethyl peroxydicarbonate initiation.[14] Copolymers of TFE−VAc were synthesized with a TFE molar composition from 7 to 63.3%.

Characterization. Polymer molar mass was characterized by a GPC (Waters U6K Injector, 510 pump) equipped with a refractive index detector (Waters 2410) and a series of Ultrastyragel columns (Waters 10^6, 10^4, and 500 Å). Using ethyl acetate or tetrahydrofuran (THF) as the mobile phase at a flow rate of 1 mL/min, polymer molar masses were calculated relative to polystyrene standards. ^{1}H and ^{19}F NMR spectra (Varian Gemini spectrometer) were obtained in $CDCl_3$ at 300.75 and 282.33 MHz, respectively. Elemental analysis was conducted by Guelph Analytical Laboratory Service (Ontario, Canada). Carbon, hydrogen, and oxygen content were measured via combustion analysis (ASTM D5373/D5291), while fluorine content was determined using the oxygen bomb combustion technique (ASTM D3761). Glass transition temperatures (T_g) were measured using a differential scanning calorimeter (DSC, Q1000), under an inert nitrogen atmosphere, with a heating rate of 10 °C/min and a scanning range of −20 to 100 °C.

The phase behavior of mixtures of CO_2 with copolymers of low TFE concentration (11.6−26.5 mol %) was studied using a variable-volume view cell. Known amounts of the solid poly(TFE-*co*-VAc), ±0.001 g, were introduced to the sample volume of a high pressure, windowed, variable-volume view cell with the maximum working pressure of 68.9 MPa and a maximum working volume of 120 cm^3 (DBR Design & Manufacturing Inc., model no. PVT-0150-100-200-286-155). Although there is a very small dead volume (0.02 cm^3) at the top of the sample volume, the entire contents of the sample volume can still be observed because the apparatus can be inverted. After the sample volume was purged with CO_2 at 0.2 MPa, the volume of the cell was minimized. High-pressure liquid CO_2 (25 °C, 13.79 MPa) was then introduced to the sample volume as the silicone oil overburden fluid was withdrawn at the equivalent flow rate using a dual-proportioning positive displacement pump (DBR Design & Manufacturing Inc., model no. PMP-0500-2-10-MB-316-M4-C0/PC). This technique facilitated the isothermal, isobaric addition of a known volume of CO_2 to within ±0.01 cm^3 into the sample volume. The mass of CO_2 was determined from the displaced volume, temperature, and pressure using an equation of state for carbon dioxide.[15] The initial concentration of each copolymer was 20 wt %. The copolymer−CO_2 mixture was then compressed to 67 MPa and mixed with a magnetically driven impeller (DBR Design & Manufacturing Inc., model no. 274152). During the compression and mixing, the poly(TFE-*co*-VAc) solubility in CO_2 was followed. If two-phase solid−liquid equilibrium was observed, then additional CO_2 was introduced to the sample volume until the copolymer concentration decreased by approximately 1 wt %. If a single, transparent phase was attained, the two-phase boundary was determined by slowly expanding the sample volume until a second phase appeared, as evidenced by the sample volume becoming opaque due to the formation of dispersed liquid copolymer droplets throughout the sample volume. The mixed phases were then allowed to separate until two transparent phases were observed. It was also determined whether the second phase was composed of solid particles or droplets of a copolymer-rich liquid phase. The appearance of a copolymer-rich liquid phase would be indicative of copolymer melting point depression in the presence of dense CO_2, a phenomenon associated with highly CO_2-soluble polymers and compounds.[16] The pressure at which the second phase appeared was considered to be a dew point if a small copolymer-rich phase settled to the bottom of the cell. Two-phase pressures were reproduced three times at each overall concentration to within approximately ±0.5 MPa using a Heise digital pressure indicator (series 9, accurate to within ±0.07 MPa for data to 68.9 MPa) and at each temperature (held to within ±0.5 °C, using a type K thermocouple).

Copolymers with higher proportions of TFE (46.7 mol %) were expected to be more difficult to dissolve in CO_2. Therefore, the phase behavior of these CO_2−copolymer mixtures was determined with equipment rated to significantly higher pressures. The apparatus and techniques used to obtain these polymer−fluid phase behavior data were described elsewhere.[10,17] The main component of the experimental apparatus was a high-pressure, variable-volume cell (Nitronic 50, 7.0 cm o.d. × 1.6 cm i.d., ∼30 cm^3 working volume). The cell was first loaded with a measured amount of copolymer to within ±0.002 g. To remove entrapped air, the cell was degassed very slowly at pressures less than 0.028 MPa with the CO_2. CO_2 was then transferred into the cell gravimetrically to within ±0.02 g using a high-pressure bomb. The mixture in the cell was viewed with a borescope (Olympus Corp., model no. F100-024-000-55) placed against a sapphire window secured at one end of the cell. A stir bar activated by a magnet located below the cell mixed the contents of the cell. The solution temperature was held to within ±0.3 °C, as measured with a type K thermocouple. A fixed copolymer concentration of approximately 5 wt % was used for each constant-concentration, phase boundary curve. The mixture in the cell was compressed to a single phase, and the pressure was then slowly decreased until a second phase appears. The transition was a cloud point if the solution becomes so opaque that it was no longer possible to see the stir bar in solution. These cloud points had been compared in our laboratories to those obtained using a laser light setup where the phase transition was the condition of 90% reduction in light transmitted through the solution. Both methods gave identical results within the reproducibility of the data. The cloud-point transitions at this concentration were expected to be close to the maximum in the pressure−composition isotherms.[18−20] The system pressure was measured with Heise pressure gauges accurate to within ±0.07 MPa for data to 69 MPa and to within ±0.35 MPa for data from 69 to 276 MPa. Cloud points were reproduced two to three times to within approximately ±0.42 MPa.

Molecular Modeling Theory

Although the interplay of solute−solute, solute−solvent, and solvent−solvent interactions should be completely considered when the dissolution behavior of

polymers in CO_2 is being explored, we realize that the polymer−polymer interactions are also of great importance in determining the solubility of the polymer. However, the interaction energies between polymer segments cannot be computed at the same level of theory as the segment−CO_2 interactions because two polymer segments have too many atoms. If we use a lower level of theory, such as DFT, then the answers would be largely meaningless. To perform these calculations, better computational algorithms and faster computers are needed to develop. Therefore, we only calculated and estimated the binding energies between polymer segment and CO_2.

There have been a number of different efforts to model the thermodynamic properties of polymer−CO_2 mixtures. Generally speaking, these modeling techniques fall into three categories: equation-of-state modeling,[21−23] statistical mechanical simulations,[24] and ab initio calculations.[12,25−27] Equation-of-state methods have not proved to be accurate enough to predict the phase behavior of polymer−CO_2 mixtures.[22] In principle, one could compute virtually all the thermodynamic properties of polymer−CO_2 mixtures through statistical mechanical simulations. However, this requires very accurate molecular interaction models, which are currently not available, especially for the CO_2−polymer cross-interactions. Another alternative is to bypass the use of potential models and directly use ab initio methods to generate the forces required for a simulation, such as is done in quantum molecular dynamics,[28−30] but this is impractical for polymer−CO_2 mixtures because of the large system sizes and weak interactions among the molecules. Weak interactions (such as dispersion or van der Waals forces) are difficult to compute from ab initio methods because high-level methods and large basis sets are needed to capture electron dispersion. Computationally efficient methods, such as density functional theory, are known to be generally inadequate for computing van der Waals interactions.[31−35] The Møller−Plesset (MP) perturbation method for including electron correlation has been used for weakly interacting systems but is known to have convergence problems.[36−38] MP2 (second-order Møller−Plesset perturbation theory) is the lowest order MP theory and is not generally adequate for computing intermolecular interaction energies, except when a substantial electrostatic interaction is involved.[39,40] Methods that include triple excitations, e.g., fourth-order Møller−Plesset with single, double, triple, and quadruple excitations MP4 (SDTQ), or coupled cluster with perturbational triples, CCSD(T), are required for many applications.[36,37,41] However, recent work indicates that failure of MP2 may in part be due to basis set superposition error.[38,42]

In this work we perform MP2 calculations to compute the interaction energies of CO_2 with various polymer fragments. Our aim is to determine the role of fluorine atoms in the backbone of the polymer on enhancing the solubility of the fluorinated copolymers in CO_2. We expect the MP2 method to be adequate for our purposes because we are interested in relative interaction energies for CO_2 on fluorinated and nonfluorinated polymer moieties; relative energies are expected to be more accurate than absolute energies. Furthermore, the presence of fluorine atoms on the polymer should increase the relative importance of electrostatic interactions, making the problem more appropriate for the MP2 method. Our previous calculations indicate that MP2 energies are fairly close to CCSD(T) energies for similar systems.[43]

Table 1. Bulk Analysis of TFE−VAc Copolymers

TFE in feed (mol %)	yield (wt %)	TFE in the copolymers (mol %)[a]	T_g (°C)	M_w/M_n/PDI (kg mol^{-1})
17.6	80	11.6	37.2	140/42/3.2
23.6	80	19.3	36.8	156/49/3.1
35.6	86	26.5	36	166/61/2.7
53.7	78	46.7	37	180/55/3.1
67.7	79	63.3	37	290/157/1.84[b]

[a] Determined from mol % C elemental analysis. [b] Measured using ethyl acetate as mobile phase. Entries 1−4 were subsequently evaluated after the mobile phase was changed to THF.

It is not possible to explicitly perform ab initio calculations on a polymer because of the large number of atoms. We therefore break the copolymer into small model segments. We then compute optimized geometries and binding energies for CO_2 interacting with these model segments. We performed geometry optimizations at the MP2/6-31+g(d) level of theory for a number of different polymer segment/CO_2 dimers. This relatively small basis set was used to make the optimizations feasible on the available computing resources. The optimized configurations were then used to calculate the more accurate single-point binding energies at larger basis set, aug-cc-pVDZ. This basis set still has significant basis set superposition error (BSSE), which is the spurious lowering of the binding energy due to the use of incomplete basis set. We have used standard counterpoise (CP) corrections[44] to approximately account for BSSE. The binding energy was computed from the supermolecule approach

$$E_b = E(12) - E(1) - E(2) \qquad (1.1)$$

where E_b is the binding energy, $E(12)$ is the total energy of the dimer (CO_2 + polymer segment), and $E(i)$ is the energy of the isolated CO_2 or polymer segment molecule. Binding energies defined in this way are negative for energetically favorable dimers. We use the average of the raw and CP corrected interaction energies as an approximation to the complete basis set limit interaction energies. We do this to avoid the computationally expensive complete basis set extrapolation. This method has been tested by us previously[43] for similar systems and found to be in good agreement with the results of Feller and Jordan.[45] All binding energies reported in this paper are averages of the MP2/aug-cc-pVDZ corrected and uncorrected interaction energies. We have computed localized charge distributions for several of the model polymer segments using the NBO method. All calculations were performed with the Gaussian 98 package, revision A11.[46]

Results

Experimental Results. A series of TFE-*co*-VAc copolymers were synthesized in supercritical CO_2 and characterized for yield, bulk composition, molar mass, and T_g, the results of which are summarized in Table 1. As shown, a series of copolymer compositions were prepared where monomer feed composition influenced polymer composition, from 11.6 to 63.3 mol % TFE. The yield (based on mass) was high for all compositions between 78 and 86%. The T_g was similar for all samples between 36 and 38 °C, which is similar to that of PVAc (38 °C). Since we were interested in comparing solubility in CO_2 as a function of copolymer composition, the

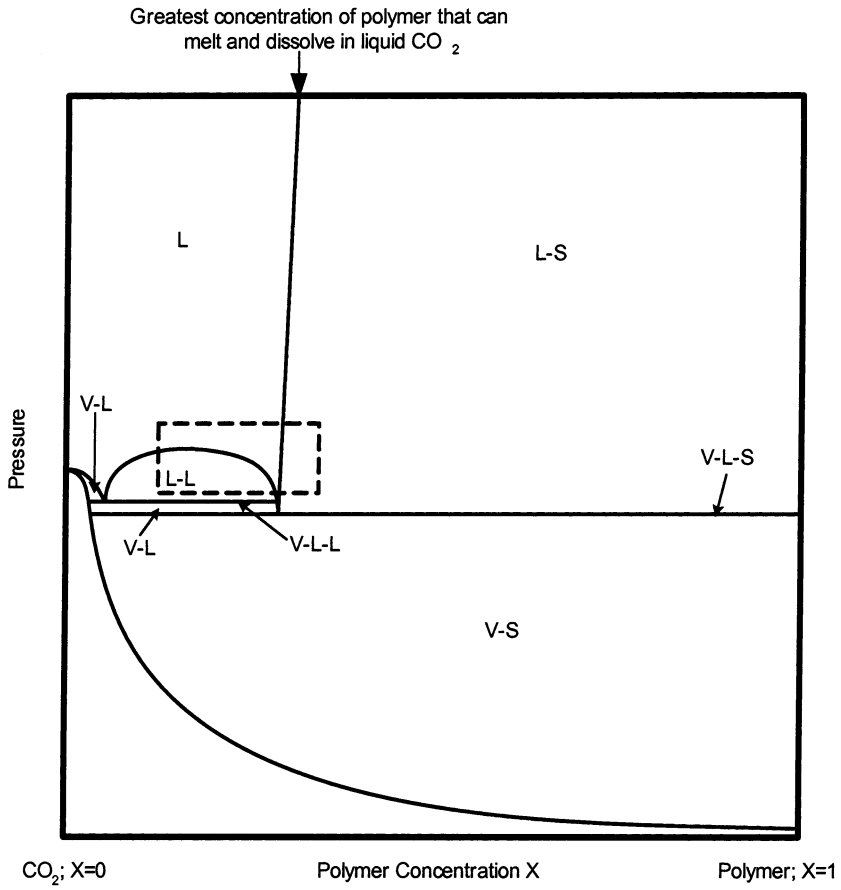

Figure 1. General pressure−composition ($P-x$) phase diagram for CO_2 and solid CO_2-philic compounds or polymers.

samples were synthesized in such a manner to yield similar molecular weight characteristics, with M_w between 140 and 180 kg/mol and the polydispersity index (PDI) between 2.7 and 3.1. For 63.3 mol % TFE copolymer, however, M_w was higher and PDI lower than the other samples. It is important to note that this sample was measured by GPC in ethyl acetate whereas the other polymers were measured in THF. Ethyl acetate may have affected the hydrodynamic radius of the copolymer differently from THF, thereby accounting for the greater M_w and smaller PDI.

The phase behavior of poly(TFE-*co*-VAc)−CO_2 mixtures was strongly influenced by the copolymer composition. (The copolymer will hereafter be designated as TFE-*co*-VAc, with the value of the TFE subscript corresponding to the mole fraction of that monomer.) The three copolymers with the smallest proportion of TFE, $TFE_{11.6}$-*co*-VAc, $TFE_{19.3}$-*co*-VAc, and $TFE_{26.5}$-*co*-VAc, melt-flowed in CO_2 when heated above their T_g's, as did the PVAc homopolymer (these are amorphous polymers). Like PVAc, these copolymers dissolved in the presence of liquid CO_2, and the general nature of the corresponding pressure−composition ($P-x$) diagram for such systems is illustrated in Figure 1.[16] (Although this figure strictly applies to binary systems in which no CO_2 dissolves in a monodisperse crystalline polymer, the region bounded by the dashed line in Figure 1 illustrates the qualitative features of the mixtures of CO_2 with the polymers used in this study.) The small box within Figure 1 illustrates the region where the CO_2-rich liquid-polymer-rich liquid data were measured. The results, shown in Figure 2, indicate that these three TFE−VAc copolymers are more CO_2-soluble than PVAc as evidenced by the cloud-point curves of these copolymers being comparable to one another and being 10 MPa lower than the PVAc cloud-point curve. Furthermore, a single phase could not be achieved at a PVAc concentration of 6 wt % at the pressure limit of 67 MPa. The greatest concentrations of the (TFE-*co*-VAc) polymers that could be attained in liquid CO_2 at the same pressure limit of 67 MPa were 7.5, 10, and 8 wt % for the $TFE_{11.6}$-*co*-VAc, $TFE_{19.3}$-*co*-VAc, and $TFE_{26.5}$-*co*-VAc polymers, respectively. These results indicate that $TFE_{19.3}$-*co*-VAc is close to the optimal composition for CO_2-solubility. These results also suggest that copolymers with a small proportion of TFE are not as likely to form TFE crystalline segments having variable lengths of CF_2 units that inhibit solubility in CO_2.

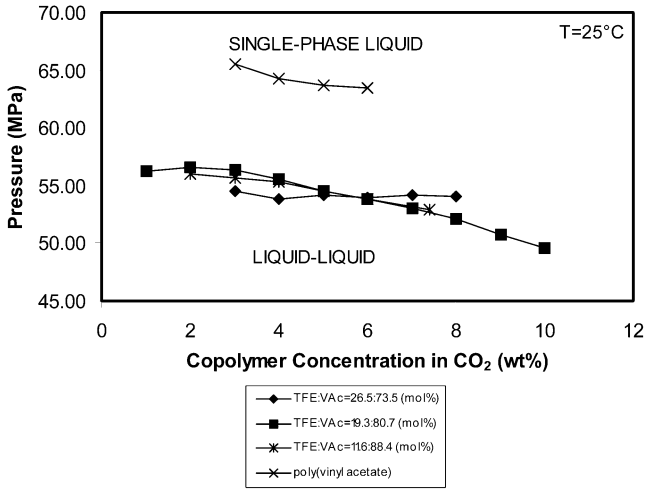

Figure 2. Pressure−composition phase diagram for CO_2 + TFE−VAc copolymer system at 25 °C.

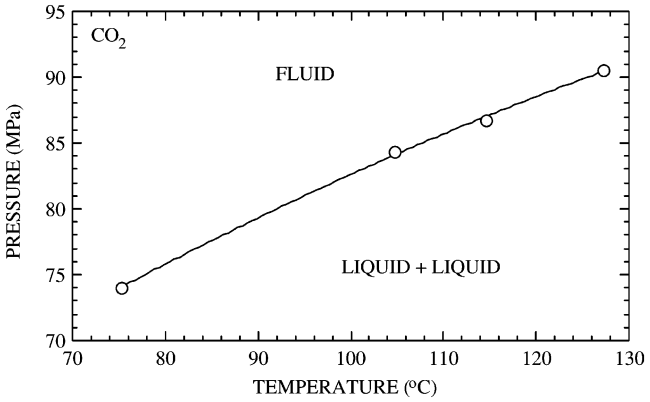

Figure 3. Cloud-point curve for ~5 wt % CO_2 + $TFE_{46.7}$-*co*-VAc system.

Because of the relatively low TFE content and copolymerization technique, the probability of lengthy block segments of TFE is low in these copolymers, and hence the propensity to crystallize and form CO_2-insoluble polymers is low.

The copolymers with higher concentrations of TFE, $TFE_{46.7}$-*co*-VAc, and $TFE_{63.3}$−VAc were markedly less CO_2-soluble. $TFE_{46.7}$-*co*-VAc was insoluble in CO_2 at temperatures below 75 °C, which is notably less CO_2 soluble than the three copolymers with lower TFE concentrations; however, the copolymer did dissolve at elevated temperatures. At a copolymer concentration of 5 wt % in CO_2—a representative mixture composition that typically yields a cloud point pressure at or near the maximum cloud-point pressure of this portion of the phase diagram—cloud-point pressures were observed at higher temperatures. The cloud point pressure was found to be 74 MPa at 75 °C and 91 MPa at 128 °C (see Figure 3). However, $TFE_{63.3}$-*co*-VAc does not dissolve in CO_2 even at 144 °C and 210 MPa. This may be due in part to the increased crystallinity of the copolymer associated with TFE-rich regions or blocks.

Molecular Modeling Results. We have employed ab initio molecular modeling to identify reasons for the enhanced solubility of TFE-*co*-VAc relative to the PVAc homopolymer. Figure 4b illustrates that the fluorinated carbons in the copolymer backbone will be adjacent to either a methylene carbon or a methyne carbon from which the pendant $-OCOCH_3$ group extends. We take one representative portion of TFE-*co*-VAc with a relatively small concentration of TFE shown in Figure 4c and divide it into three small molecules, shown in Figure 4d, which are conducive to molecular modeling calculations. First, we cut the molecule between the two CF_2 functional groups, yielding two fluorous molecules, 3,3,3-trifluoroisopropyl acetate (TFIPA) and 4,4,4-trifluoro-*sec*-butyl acetate (TFSBA). The third small molecule is 2,2,3,3-tetrafluorobutane (FB), which is a model for the backbone of the polymer. The hydrocarbon analogues of these small molecules, shown in Figure 4e, are isopropyl acetate (IPA), *sec*-butyl acetate (SBA), and *n*-butane. These molecules are used for direct comparisons with the semifluorinated compounds.

We have identified four possible binding configurations for CO_2 interacting with TFIPA and TFSBA. We use the TFIPA molecule as an example to illustrate the possible binding configurations because TFSBA has similar CO_2 binding configurations. The specific binding configurations are illustrated in Figure 5 as (A) ester oxygen, (B) carbonyl oxygen, tilted toward the methyl

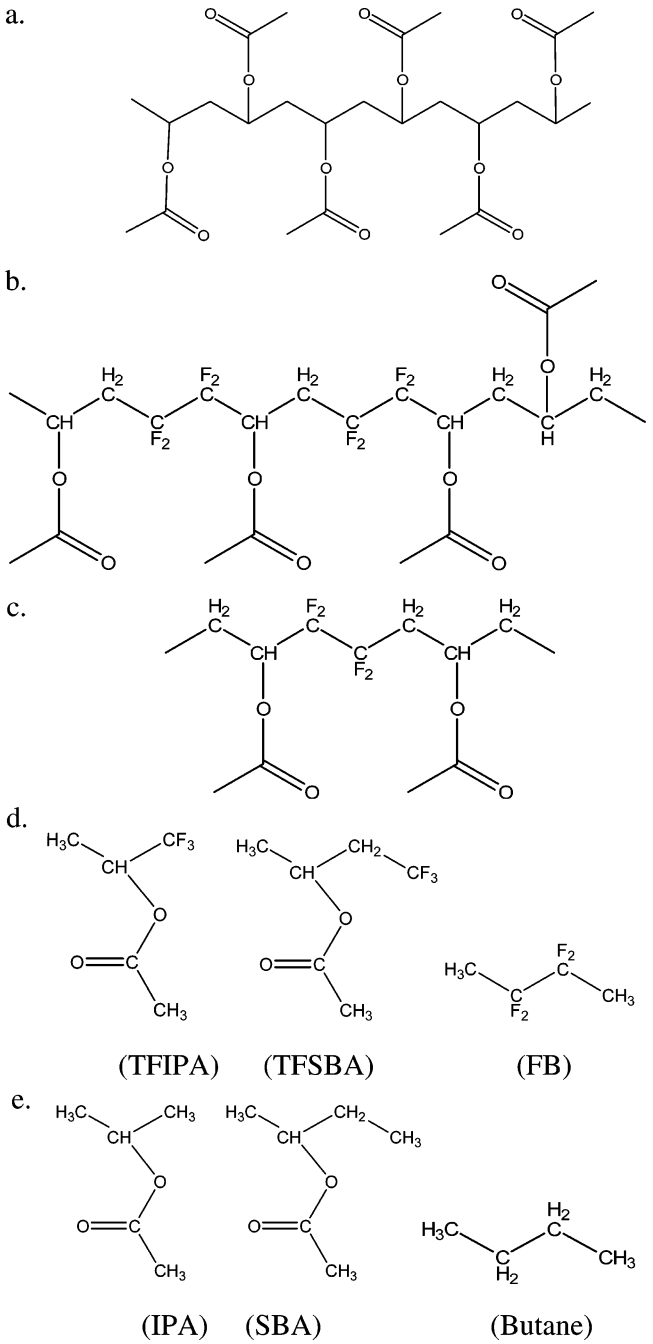

Figure 4. (a) PVAc; (b) a portion of poly(TFE-*co*-VAc) that lacks TFE block segments; (c) a representative segment of this copolymer; (d) the three small molecules used in molecular modeling that capture the features of the copolymer: trifluoroisopropyl acetate, trifluoro-*sec*-butyl acetate, and tetrafluorobutane; (e) the hydrocarbon analogues of the small fluorous molecules: isopropyl acetate, *sec*-butyl acetate, and *n*-butane.

group, (C) carbonyl oxygen, tilted toward the ester group, and (D) backbone fluorine atoms. Geometry optimizations were started by placing the CO_2 molecule at various positions around the TFIPA and TFSBA molecules. From five to eight different starting geometries were used for each of the polymer fragments. The hydrocarbon analogues, IPA and SBA, were studied in the same way.

TFIPA/CO_2 and IPA/CO_2. Binding configuration A has an interaction energy of −15.9 kJ/mol. The optimized geometry for binding configuration A is shown in Figure 6. The dashed lines indicate interaction points between the two molecules. The atom−atom distances

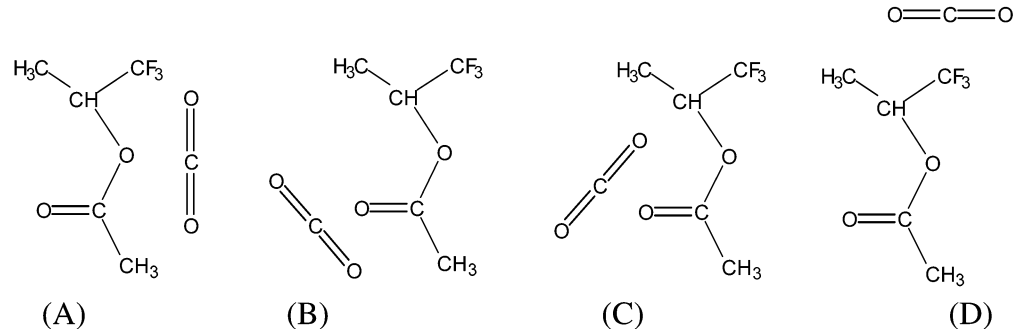

Figure 5. Four distinct binding configurations for TFIPA and a single CO_2 molecule. (A) Binding with the ester oxygen. (B) Binding with the carbonyl oxygen, tilting toward the methyl group. (C) Binding with the carbonyl oxygen, tilting toward the ester group side. (D) Binding with the fluorine atoms in the backbone.

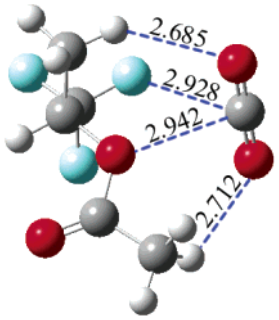

Figure 6. Binding interactions of TFIPA/CO_2 for configuration A. The distances are in angstroms.

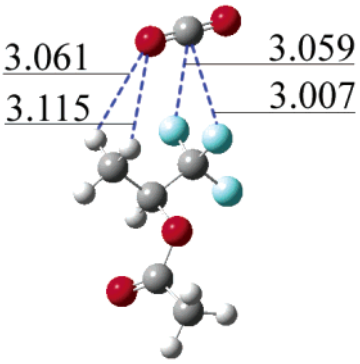

Figure 7. Binding interactions of TFIPA/CO_2 for configuration D. Distances are in angstroms.

in angstroms are also shown. The carbon atom of the CO_2 molecule binds with both the fluorine atom and the ester oxygen atom on TFIPA in this configuration. Each oxygen on CO_2 interacts with a hydrogen in what can be termed a weakly hydrogen-bonding configuration.[27] We identify configuration A as quadradentate binding because the CO_2 molecule has four interaction points with the polymer moiety. In configurations B and C, the CO_2 molecule mainly interacts with the carbonyl oxygen atom of the TFIPA. This gives interaction energies that are quite similar to those between IPA and CO_2. Figure 7 shows the interactions for configuration D. This is also a quadradentate binding configuration. The carbon of the CO_2 interacts with two fluorine atoms while one oxygen of the CO_2 interacts with two hydrogens.

The binding energies for the four TFIPA/CO_2 binding configurations are listed in Table 2, along with the interaction energies for CO_2 with the hydrocarbon analogue, IPA. There is a difference of about 1.2 kJ/mol between the binding energies of TFIPA/CO_2 and IPA/CO_2 for configurations A and B. This energy difference is within the estimated accuracy of the ab initio

Table 2. Binding Energies for TFIPA/CO_2 and IPA/CO_2 at Each of the Four Binding Configurations of Figure 3[a]

binding configurations	binding energies (kJ/mol)	
	TFIPA/CO_2	IPA/CO_2
A	−15.9	−14.7
B	−13.0	−14.2
C	−15.9	−15.9
D	−9.6	no minimum

[a] Geometries optimized at the MP2/6-31+g(d) level of theory with binding energies computed at MP2/aug-cc-pVDZ.

calculations. The limited accuracy is due to lack of convergence in the theoretical method (MP2) and the choice of basis set. Thus, we conclude that the fluorine atoms on the polymer backbone do not substantially affect (positively or negatively) the binding energies of CO_2 with the acetate side chain.

We have not been able to find a configuration D for the IPA/CO_2 system, even though we started from several different initial configurations. In every case, the CO_2 molecule always migrates around the molecule to bind with the carbonyl or ester oxygen of the IPA molecule. This implies that there is no minimum corresponding to binding configuration D for the IPA/CO_2 system. However, the D geometry of the TFIPA/CO_2 system shows a considerable binding energy of −9.6 kJ/mol. This additional binding site for the TFIPA/CO_2 system is probably one of the main reasons for the increase in solubility of the TFE-*co*-VAc molecule in CO_2. Note that configuration D requires a junction between fluorinated and nonfluorinated segments. We estimate that at least two CO_2 molecules can favorably interact with each CF_2−CH_2 junction. Clearly, a moderate fraction of TFE in the copolymer would favor higher CO_2 solubility, since the number of CF_2−CH_2 junctions per polymer molecular weight is maximized for moderate mole fractions of TFE.

TFSBA/CO_2 and SBA/CO_2. The TFSBA/CO_2 system was investigated using similar binding configurations from A to D of the TFIPA/CO_2 system. The SBA/CO_2 system was used for comparison. Table 3 lists the calculated binding energies for these systems. The calculations for TFIPA/CO_2 and IPA/CO_2 indicate that the binding energies for configurations B and C should be similar for the fluorinated and nonfluorinated segments. We therefore did not calculate binding energies for configurations B and C for the SBA/CO_2 system. We used the values of the binding energies for configurations B and C from the IPA/CO_2 system as an estimate for the binding energies for SBA/CO_2 for the same configurations. The binding energy of configuration A for TFSBA/CO_2 is −18.8 kJ/mol, which is much larger

Table 3. Binding Energies for TFSBA/CO_2 and SBA/CO_2 at Each of the Four Binding Configurations of Figure 3[a]

binding configurations	binding energies (kJ/mol)	
	TFSBA/CO_2	SBA/CO_2
A	−18.8	−16.3
B	−13.8	−14.2[b]
C	−15.5	−15.9[b]
D	−11.7	no minimum

[a] Geometries optimized at the MP2/6-31+g(d) level of theory with binding energies computed at MP2/aug-cc-pVDZ. [b] Estimated from IPA/CO_2 calculations.

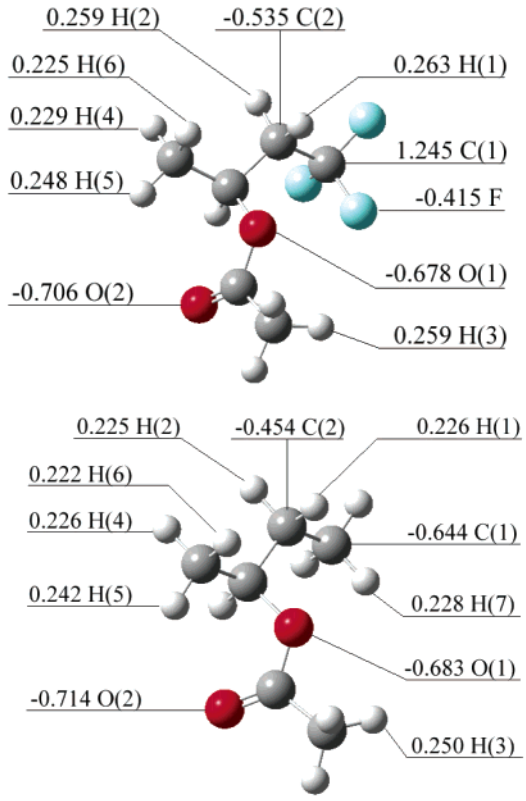

Figure 8. Charge distribution on the TFSBA (top) and SBA (bottom) molecules.

than the binding energies for any site of any of the other systems. Note from Table 3 that the interaction energy for configuration A of TFSBA is 2.5 kJ/mol more attractive than for SBA. This difference is larger than the expected uncertainty in the calculations.

We have examined the NBO charge distributions of TFSBA and other molecules in order to determine the origin of the enhanced binding for configuration A of TFSBA/CO_2. The local charges on atoms of TFSBA are shown in Figure 8. Note that the charge on hydrogens H(1) and H(2) is about 0.26. This is significantly larger than on hydrogens in the same positions on SBA or on hydrocarbons, which is about 0.23. Thus, hydrogens H(1) and H(2) are more acidic than typical hydrocarbon hydrogens. This is due to the fact that they are on the carbon that is beta to the highly electronegative fluorines. Configuration A on TFSBA/CO_2 is a quadradentate binding site, with one CO_2 oxygen interacting with H(1). The acidic hydrogen acts as a better Lewis acid for the CO_2 oxygen Lewis base. This, we believe, is the reason for the enhanced binding of configuration A for TFSBA/CO_2.

The charges on the two oxygen atoms of TFSBA are very similar to those of SBA. This is why the binding

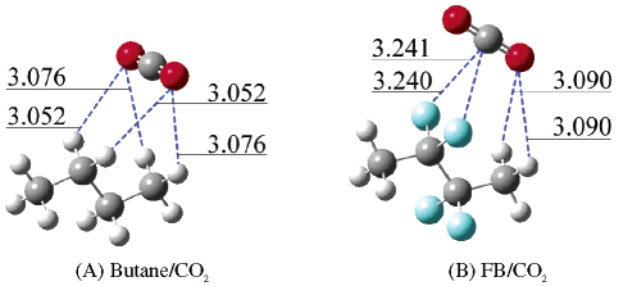

Figure 9. Optimized binding geometries for the *n*-butane/CO_2 (A) and FB/CO_2 (B) systems. Distances are in angstroms.

energies of configurations B and C are very similar for all the systems studied. Configuration D for the TFSBA/CO_2 system has a binding energy of −11.7 kJ/mol. This is larger than that for the same configuration on TFIPA/CO_2. We believe that the increase in binding energy is again due to the increased acidity of the hydrogens on the backbone. Note that our calculations could not locate a minimum for configuration D for SBA/CO_2, as was the case for IPA/CO_2.

FB/CO_2 and Butane/CO_2. To further investigate the interactions between the CO_2 molecule and the backbones of the polymers, FB and butane are used as models of the fluorinated and nonfluorinated backbones, respectively. Starting from several initial configurations, we identified a single geometry with the strongest interaction for each of the systems. Figure 9 shows the optimized binding geometries for the systems. The binding energies for butane/CO_2 and FB/CO_2 are −8.4 and −12.1 kJ/mol, respectively. The FB/CO_2 binding energy is 3.7 kJ/mol larger in magnitude than that for butane/CO_2. The hydrogen atoms involved in the interactions of the FB/CO_2 system are more acidic than those on typical hydrocarbons. The FB hydrogens have a charge of 0.256, compared with 0.216 for hydrogens on butane. The FB/CO_2 binding energy is close to the configuration D binding energy for TFSBA/CO_2 of −11.7 kJ/mol but stronger than that for TFIPA/CO_2 of −9.6 kJ/mol. The hydrogen atoms involved in the configuration D interactions have charges of 0.26 and 0.24 for TFSBA/CO_2 and TFIPA/CO_2 systems, respectively. These values are close to those for the FB/CO_2 system, indicating that the FB molecule is a reasonable surrogate for the backbone of the polymer. The enhanced binding of CO_2 with the semifluorinated molecules relative to nonfluorinated compounds indicates that the backbone of the semifluorinated polymers acts as effective simultaneous Lewis acids (H−O) and Lewis bases (F−C) toward CO_2. These interactions are likely to significantly enhance the solubility of the polymer compared with nonfluorinated analogues. Note also that the acidic hydrogens are only available on semifluorinated backbones. This corroborates the experimental observation that high fractions of TFE in the copolymer reduce the solubility.

Discussion

A CO_2 molecule can act simultaneously as both a Lewis acid and a Lewis base if the molecule with which it is interacting has both Lewis base and acid groups. Our molecular modeling results show that this is precisely the case for semifluorinated polymers such as TFE−VAc. Perfluorinated polymers lack Lewis acid sites and also exhibit very high melting points. Furthermore, O−F interactions are only weakly attractive

since both the oxygens in CO_2 and the fluorine in the polymer are electron-rich.[25] This is one of the major reasons that partially fluorinated polymers are more CO_2-philic than perfluorinated ones. Raveendran et al.[12] have also observed enhanced binding of CO_2 with partially fluorinated molecules. They performed ab initio calculations on $CO_2-CF_nH_{4-n}$ for $n = 0-4$. They concluded that there may be an optimal density of fluorine atoms in a molecule leading to maximum CO_2-phicility.[12] They attribute this optimal density to the competition among the individual electronegative fluorine atoms. In other words, fluorine atoms in highly fluorinated molecules are less effective electron donors. We believe this effect to be of minor importance compared with the requirement for a molecule to have both Lewis acid and base sites present in the correct geometry to interact simultaneously with CO_2. This is difficult to achieve in a small molecule like CF_nH_{4-n}. We note that Fried and Hu have also studied the binding of CO_2 on semifluorinated small molecules using ab initio calculations.[47] They found that quadrupole−dipole interactions between CO_2 and the partially fluorinated molecules contribute significantly to the total interaction energy.[47] Their results are in agreement with our calculations, showing that partially fluorinated molecules should be more soluble than perfluorinated species.

Another consideration is Wallen's claim that fluorination of methane makes the hydrogen atoms less acidic compared with hydrogen atoms in methane.[12] This is not the case for larger molecules. The hydrogen atoms on the carbon β to the fluorine atom are more acidic than the hydrogens on *n*-butane. NBO charges for hydrogens on FB and butane are about 0.26 and 0.22, respectively. The enhancement of H atom acidity relative to the hydrocarbon cannot be observed by studying semifluorinated methane.

Binding of CO_2 to carbonyl functional groups is virtually unaffected by the fluorination, as shown in Table 2. In contrast, Raveendran et al. noted that fluorination decreases the carbonyl CO_2-phicility of partially fluorinated acetaldehyde.[26] Separation of the fluorine atoms from the carbonyl group by more than one carbon atom mitigates the effect of the fluorine on carbonyl−CO_2 binding, however. Note that the charges on the ester and carbonyl oxygens in both TFSBA and SBA are almost identical, as shown in Figure 8.

Summary

High molecular weight poly(TFE-*co*-VAc) with TFE content ranging between 11.6 and 26.5 mol % required lower pressure for dissolution in CO_2 at 25 °C and at low concentrations (<6 wt %) than PVAc homopolymer. Further, these poly(TFE-*co*-VAc) copolymers were soluble to higher concentrations in CO_2 (7.4−10 wt %) than PVAc (6 wt %). The copolymer composed of 46.7 mol % TFE was not soluble in CO_2 at 25 °C but was CO_2-soluble at temperatures greater than 75 °C. The copolymer with 63.3 mol % TFE was insoluble in CO_2 at all conditions, possibly due to the presence of TFE blocks, which may be crystalline and thereby reduce solubility. Introduction of hexafluoropropylene units may disrupt this apparent crystallinity while maintaining the fluorocarbon content and enhancing CO_2-solubility.

Ab initio calculations have revealed the following reasons for the increased solubility of poly(TFE-*co*-VAc) relative to PVAc. (1) The specific geometry and functionality of the polymer give rise to "quadradentate" binding of CO_2 to the polymer, having an interaction energy about 2.5 kJ/mol more favorable than the nonfluorinated analogue; compare configurations A in Table 3. (2) The interaction of CO_2 with the partially fluorinated backbone is 3.7 kJ/mol more favorable than with the hydrocarbon analogue. (3) The electron-withdrawing effects of the F atoms on the backbone renders nearby H atoms slightly more acidic, promoting stronger hydrogen bonding with the O atoms in CO_2. Finally, we note that CO_2 acts simultaneously as both a Lewis acid and a Lewis base for many of the binding geometries identified through molecular modeling.

Acknowledgment. We are grateful to the following agencies for partial support of this research: Natural Sciences and Engineering Research Council of Canada (M.S.S.), National Science Foundation (R.M.E.), and DOE National Energy Technology Laboratory and National Petroleum Technology Office (R.M.E.). Polymer syntheses were performed at the University of Toronto, ultrahigh-pressure phase behavior measurements were taken at VCU, and computations were performed at the University of Pittsburgh Center for Molecular and Materials Simulations.

References and Notes

(1) Jones, C. W. United States Patent 5,723,556. 1998.
(2) Feiring, A. E.; Wonchoba, E. R. *Macromolecules* **1998**, *31*, 7103−7104.
(3) Kogel, H. C.; Vollmar, J. F.; Proschek, P.; Mager, B.; Scharf, G.; Buttel, H. M. In *Prosthetic Substitution of Blood Vessels: Actual State and Future Development*; Kogel, H. C., Ed.; Quintessenz: Munich, 1991; p 143.
(4) Lousenberg, R. D.; Shoichet, M. S. *Macromolecules* **2000**, *33*, 1682−1685.
(5) Baradie, B.; Shoichet, M. S. *Macromolecules* **2002**, *35*, 3569−3575.
(6) Rindfleisch, F.; DiNoia, T. P.; McHugh, M. A. *J. Phys. Chem.* **1996**, *100*, 15581−15587.
(7) Shen, Z.; McHugh, M. A.; Xu, J.; Belardi, J.; Kilic, S.; Mesiano, A.; Bane, S.; Karnikas, C.; Beckman, E. J.; Enick, R. M. *Polymer* **2003**, *44*, 1491−1498.
(8) Tuminello, W. H.; Brill, D. J.; Walsh, D. J.; Paulaitis, M. E. *J. Appl. Polym. Sci.* **1995**, *56*, 495−499.
(9) Kirby, C. F.; McHugh, M. A. *Chem. Rev.* **1999**, *99*, 565−602.
(10) Mertdogan, C. A.; Byun, H. S.; McHugh, M. A.; Tuminello, W. H. *Macromolecules* **1996**, *29*, 6548−6555.
(11) Mertdogan, C. A.; DiNoia, T. P.; McHugh, M. A. *Macromolecules* **1997**, *30*, 7511−7515.
(12) Raveendran, P.; Wallen, S. L. *J. Phys. Chem. B* **2003**, *107*, 1473−1477.
(13) Hunadi, R. J.; Baum, K. *Synthesis* **1982**, *39*, 454.
(14) Strain, F.; Bissinger, W. E.; Dial, W. R.; Rudoff, H.; DeWitt, B. J.; Stevens, H. C.; Langston, J. H. *J. Am. Chem. Soc.* **1950**, *72*, 1254−1263.
(15) Span, R.; Wagner, W. *J. Phys. Chem. Ref. Data* **1996**, *25*, 1509−1596.
(16) Hong, L.; Thies, M. C.; Enick, R. M. *J. Supercrit. Fluids*, in press.
(17) Meilchen, M. A.; Hasch, B. M.; MeHugh, M. A. *Macromolecules* **1991**, *24*, 4874−4882.
(18) Allen, G.; Baker, C. H. *Polymer* **1965**, *6*, 181−191.
(19) Irani, C. A.; Cozewith, C. *J. Appl. Polym. Sci.* **1986**, *31*, 1879−1899.
(20) Lee, S. H.; Lostracco, M. A.; Hasch, B. M.; McHugh, M. A. *J. Phys. Chem.* **1994**, *98*, 4055−4060.
(21) Luna-Barcenas, G.; Mawson, S.; Takishima, S.; DeSimone, J. M.; Sanchez, I. C.; Johnston, K. P. *Fluid Phase Equilib.* **1998**, *146*, 325−337.
(22) Lora, M.; Rindfleisch, F.; McHugh, M. A. *J. Appl. Polym. Sci.* **1999**, *73*, 1979−1991.
(23) Lora, M.; McHugh, M. A. *Fluid Phase Equilib.* **1999**, *157*, 285−297.
(24) Cui, S. T.; Cochran, H. D.; Cummings, P. T. *J. Phys. Chem. B* **1999**, *103*, 4485−4491.
(25) Diep, P.; Jordan, K. D.; Johnson, J. K.; Beckman, E. J. *J. Phys. Chem. A* **1998**, *102*, 2231−2236.

(26) Raveendran, P.; Wallen, S. L. *J. Am. Chem. Soc.* **2002**, *124*, 7274−7275.
(27) Raveendran, P.; Wallen, S. L. *J. Am. Chem. Soc.* **2002**, *124*, 12590−12599.
(28) Gross, A.; Scheffler, M. *Phys. Rev. B* **1998**, *57*, 2493−2506.
(29) Remler, D. K.; Madden, P. A. *Mol. Phys.* **1990**, *70*, 921−966.
(30) Car, R.; Parrinello, M. *Phys. Rev. Lett.* **1985**, *55*, 2471−2474.
(31) Wesolowski, T. A. *J. Chem. Phys.* **2000**, *115*, 1666−1667.
(32) Wu, X.; Vargas, M. C.; Nayak, S.; Lotrich, V.; Scoles, G. *J. Chem. Phys.* **2001**, *115*, 8748−8757.
(33) Misquitta, A. J.; Szalewicz, K. *Chem. Phys. Lett.* **2002**, *357*, 301−306.
(34) Wesolowski, T. A.; Morgantini, P. Y.; Weber, J. *J. Chem. Phys.* **2002**, *116*, 6411−6421.
(35) Van Mourik, T.; Gdanitz, R. J. *J. Chem. Phys.* **2002**, *116*, 9620−9623.
(36) Tsuzuki, S.; Uchimaru, T.; Matsumura, K.; Mikami, M.; Tanabe, K. *Chem. Phys. Lett.* **2000**, *319*, 547−554.
(37) Hobza, P.; Selzle, H. L.; Schlag, E. W. *J. Phys. Chem.* **1996**, *100*, 18790−18794.
(38) Rappe, A. K.; Bernstein, E. R. *J. Phys. Chem. A* **2000**, *104*, 6117−6128.
(39) Pedulla, J. M.; Vila, F.; Jordan, K. D. *J. Chem. Phys.* **1996**, *105*, 11091−11099.
(40) Christie, R. A.; Jordan, K. D. *J. Phys. Chem. A* **2001**, *105*, 7551−7558.
(41) Woon, D. E.; Peterson, K. A.; Dunning, T. H. *J. Chem. Phys.* **1998**, *109*, 2233−2241.
(42) Hobza, P.; Havlas, Z. *Theor. Chem. Acc.* **1998**, *99*, 372−377.
(43) Kilic, S.; Michalik, S.; Wang, Y.; Johnson, J. K.; Enick, R. M.; Beckman, E. J. *Ind. Eng. Chem. Res.* **2003**, *42*, 6415−6424.
(44) Boys, S. F.; Bernardi, F. *Mol. Phys.* **1970**, *19*, 553−566.
(45) Feller, D.; Jordan, K. D. *J. Phys. Chem. A* **2000**, *104*, 9971−9975.
(46) Frisch, M. J.; Truck, G. W.; Schlegel, H. B.; Scuseria, G. E.; Robb, M. A.; Cheeseman, J. R.; Zakrzewski, V. G.; Montgomery, J. A., Jr.; Stratmann, R. E.; Burant, J. C.; Dapprich, S.; Millam, J. M.; Daniels, A. D.; Kudin, K. N.; Strain, M. C.; Farkas, O.; Tomasi, J.; Barone, V.; Cossi, M.; Cammi, R.; Mennucci, B.; Pomelli, C.; Adamo, C.; Clifford, S.; Ochterski, J.; Petersson, G. A.; Ayala, P. Y.; Cui, Q.; Morokuma, K.; Salvador, P.; Dannenberg, J. J.; Malick, D. K.; Rabuck, A. D.; Raghavachari, K.; Foresman, J. B.; Cioslowski, J.; Ortiz, J. V.; Baboul, A. G.; Stefanov, B. B.; Liu, G.; Liashenko, A.; Piskorz, P.; Komaromi, I.; Gomperts, R.; Martin, R. L.; Fox, D. J.; Keith, T.; Al-Laham, M. A.; Peng, C. Y.; Nanayakkara, A.; Challacombe, M.; Gill, P. M. W.; Johnson, B.; Chen, W.; Wong, M. W.; Andres; Gonzalez, C.; Head-Gordon, M.; Replogle, E. S.; Pople, J. A. *Gaussian 98, Revision A*; Gaussian, Inc.: Pittsburgh, PA, 2001.
(47) Fried, J. R.; Hu, N. *Polymer* **2003**, *44*, 4363−4372.

MA049384U